Preparation and Characterization of Poly(butylene terephthalate) Nanocomposites with Various Organoclays

Ashwini B. Nirukhe, V. V. Shertukde

Department of Polymer Engineering and Technology, University Institute of Chemical Technology, Matunga (E), Mumbai, India

Received 21 July 2007; accepted 27 January 2009
DOI 10.1002/app.30112
Published online 19 March 2009 in Wiley InterScience (www.interscience.wiley.com).

ABSTRACT: Layered-silicate-based polymer–clay nanocomposite materials were prepared depending on the surface modification of montmorillonite (MMT). Nanocomposites consisting of poly(butylene terephthalate) (PBT) as a matrix and dispersed inorganic clay modified with cetyl pyridinium chloride (CPC), benzyl dimethyl *N*-hexadecyl ammonium chloride, and hexadecyl trimethyl ammonium bromide by direct melt intercalation were studied. The organoclay loading was varied from 1 to 5 wt %. The organoclays were characterized with X-ray diffraction (XRD) to compute the crystallographic spacing and with thermogravimetric analysis to study the thermal stability. Detailed investigations of the mechanical and thermal properties as well as a dispersion study by XRD of the PBT/clay nanocomposites were conducted. X-ray scattering showed that the layers of organoclay were intercalated with intercalating agents. According to the results of a differential scanning calorimetry analysis, clay acted as a nucleating agent, affecting the crystallization. The PBT nanocomposites containing clay treated with CPC showed good mechanical properties because of intercalation into the polymer matrix. © 2009 Wiley Periodicals, Inc. J Appl Polym Sci 113: 585–592, 2009

Key words: fillers; organoclay; nanocomposites; nucleation

INTRODUCTION

In general, polymers find limited uses in their virgin form because of the low level of many desirable properties with respect to their end-use applications. Thus, different types of additives and fillers need to be added to virgin polymers to obtain the desired properties. One of the most promising ways of enhancing the properties of polymers is the production of polymer nanocomposites.[1]

Layered silicates dispersed in a polymer matrix as a reinforcing phase are some of the most important forms of nanocomposites, and they are categorized as polymer–clay nanocomposites. Nowadays, nanocomposites attract much attention from industrial and academic researchers; significant improvements have been shown in the physical properties of polymers, including mechanical, thermal, and gas barrier properties, with the addition of very small amounts of clay because clay possesses a high aspect ratio and platelet morphology.[2,3] Many investigations have been carried out to produce polymer–clay nanocomposites, which have included polymers such as polyamide 6,[4,5] polyethylene,[6] poly(ethylene terephthalate),[7,8] epoxy,[9] polypropylene,[10] polystyrene,[11] and unsaturated polyester.[12] Montmorillonite (MMT) has been used as a filler in many nanocomposites. Domenico[13] and Xiao et al.[14] reported the preparation of poly(butylene terephthalate) (PBT)/clay nanocomposites from thermally stable organically modified MMT.

PBT is an important semicrystalline engineering thermoplastic that has found widespread applications in electrical components, electronics, automotive parts, industrial components, appliances, and consumer items.[15] PBT possesses a fast crystallization rate, good solvent resistance, easy processability, and a low impact strength and heat distortion temperature. PBT/clay nanocomposites have been prepared via melt intercalation with the use of alkyl ammonium modified MMT. However, in the case of these nanocomposites, the high temperature that is required for melt intercalation and processing leads to decomposition of the alkyl ammonium cations in organically modified MMT. It alters the interface between the filler and polymer matrix and leads to degradation of the polymer, which decreases the desired level of the properties. Thus, the thermal stability of an intercalant is required for the proper dispersion of clay in a polymer matrix.[14]

In our work, we used three intercalating agents—cetyl pyridinium chloride (CPC), benzyl dimethyl *N*-hexadecyl ammonium chloride (BDHAC), and hexadecyl trimethyl ammonium bromide (HTAB)—to prepare different organically modified MMTs and then prepared PBT/clay nanocomposites. Nanocomposites were prepared by melt intercalation with clay loadings varying from 1 to 5 wt %. A study of

Correspondence to: V. V. Shertukde (vikrantsher@rediffmail.com).

the mechanical and thermal properties and an X-ray diffraction (XRD) study of the nanocomposites were also carried out to analyze these nanocomposites.

EXPERIMENTAL

Materials

PBT (Arnite B-600; density = 1.3 g/cc) was acquired from DSM Engineering Plastics (Pune, India). Na-MMT clay (cation-exchange capacity = 95 mequiv/100 g) was provided by Crystal Nanoclay Pvt., Ltd. (Pune, India). The intercalating agents used for modification—CPC, BDHAC, and HTAB—were supplied by S.D. Fine Chemical, Ltd. (Mumbai, India). The structures of the intercalating agents are shown in Table I.

TABLE I
Structures of the Intercalating Agents

Intercalating agent	Structure
CPC ($C_{21}H_{38}ClN$)	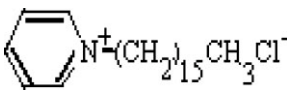
BDHAC ($C_{25}H_{46}ClN$)	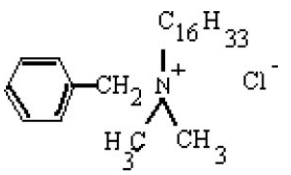
HTAB ($C_{19}H_{42}BrN$)	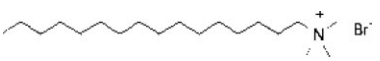

Preparation of the organically modified clay

Na-MMT (20 g; cation-exchange capacity = 95 mequiv/100 g) was dispersed in 2.5 L of distilled water at 80°C with mechanical stirring for 1 h. A solution of a calculated quantity of the intercalating agent (i.e., 8.3 g of CPC, 10.8 g of BDHAC, or 9.4 g of HTAB) in distilled water at 80°C was added to the dispersion. The resultant mixture was stirred at 80°C for 4 h. The solution was then filtered, and the organoclay was washed with distilled water 3 or 4 times to remove residual salt. The organoclay was dried in an air-circulating oven at 100 ± 5°C for 8–10 h and then ground into a powder to produce the organically modified clay. The clays treated with the intercalating agents BDHAC, CPC, and HTAB were named B-TC, C-TC, and H-TC, respectively. The untreated clay was called UNT.

Preparation of the PBT/clay nanocomposites: compounding and molding

PBT pellets were preheated at 100°C for a minimum of 4 h, and the organoclay was dried at 80°C for 2 h in an air-circulating oven before use. The PBT and organoclays were melt-compounded with a twin-screw extruder (M/s. APV Baker, Peterborough, United Kingdom; length/diameter = 25 : 1) with organoclay loadings of 1, 3, and 5 wt % with the base polymer. The extrusion was carried out with a temperature profile of 210, 230, 240, 245, and 250°C from the hopper to the die at 40 rpm. The samples were labeled with the composition and weight percentage of the organoclay (e.g., PBT/B-TC1 represents a PBT nanocomposite containing 1 wt % B-TC organoclay).

The extruded pellets were injection-molded with an injection-molding machine (M/s Boolani Engineering, Ltd., Mumbai, India) to acquire standard tensile (ASTM D 638), flexural (ASTM D 790), and notched Izod (ASTM D 256) specimens with a temperature profile of 220, 250, and 260°C from the barrel to the nozzle.

Testing and characterization

Tensile and flexural tests were performed on a universal testing machine (LR 50K, Lloyd Instruments, Ltd., Fareham, Hants, United Kingdom). Tensile and flexural properties were determined at crosshead speeds of 50 and 2.8 mm/min, respectively, at room temperature. The results reported here are averages of three successive tests. Notched Izod impact tests were performed at room temperature with an Avery Dension model 6709 (Pasadena, California) impact tester with a 5-J pendulum at a striking velocity of 3.46 m/s. The results reported here are averages of five successive tests.

The organoclay and PBT/clay nanocomposites were characterized for dispersion and thermal studies with the help of XRD, thermogravimetric analysis (TGA), and differential scanning calorimetry (DSC).

XRD

XRD experiments were performed on organoclay and PBT/clay nanocomposite specimens. XRD patterns were obtained with a Rigaku Miniflex X-ray (Geldermalsen, The Netherlands) diffractometer using Cu Kα radiation ($\lambda = 1.5406$ Å) at a generated voltage of 30 kV and at a current of 15 mA at room temperature. The diffractograms were scanned from $2\theta = 2°$ to $2\theta = 10°$ with a scanning rate of 2°/min for the organoclay and from $2\theta = 2°$ to $2\theta = 40°$ for nanocomposite specimens at the same scanning rate. Bragg's law ($\lambda = 2d \sin \theta$) was used to compute the crystallographic spacing (d) for the UNT and treated MMT.

TGA

The thermal stability was studied with TGA. The weight loss due to the formation of volatile products after degradation at a high temperature was

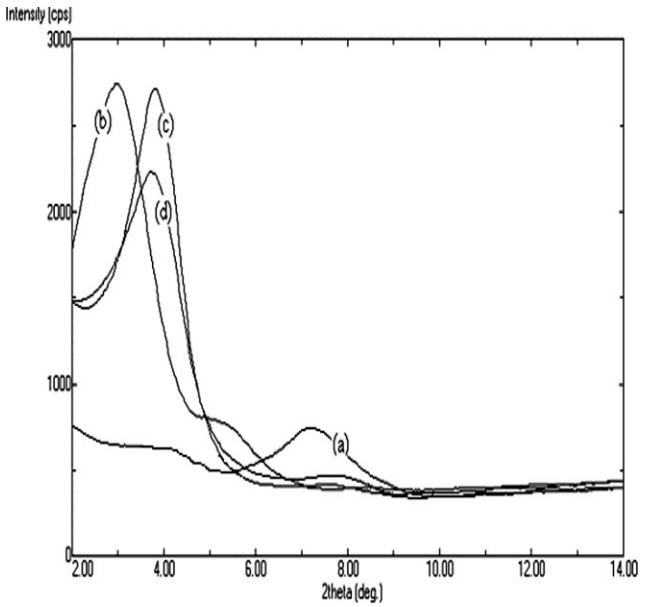

Figure 1 XRD patterns of (a) UNT, (b) B-TC, (c) C-TC, and (d) H-TC.

monitored as a function of temperature. TGA for the organoclay and Na-MMT was characterized with a TA SDT Q 600 thermogravimetric analyzer (TA Instruments, New Castle, Delawre). The samples were heated under a nitrogen atmosphere at a heating rate of 20°C/min from room temperature to 600°C.

DSC

DSC measurements were performed with a TA Q100 analyzer (TA Instruments, New Castle, Delaware). The weight of the sample (between 6 and 9 mg) was taken in a standard aluminum pan. Temperature calibration was performed with indium as a reference [melting temperature (T_m) = 156.6°C, heat flow = 2.8 J/g]. The samples were heated first to 270°C and kept there for 3 min in a hermetic cell to remove the thermal history at a rate of 20°C/min, and then they were cooled at the same rate to 20°C and again heated to 270°C under a nitrogen atmosphere. Both crystallization and melting parameters were obtained from cooling and heating scans. T_m was considered to be the maximum of the endothermic melting peak from heating scans, and the crystallization temperature (T_c) was considered the maximum of the exothermic peak of crystallization from the cooling scans.

RESULTS AND DISCUSSION

Characteristics of the organoclays

XRD measurements are shown in Figure 1. The values of 2θ and the corresponding *d*-spacings for UNT and treated clays with each intercalating agent used for the modification are presented in Table II.

TABLE II
***d*-Spacing for the UNT and Treated Clays**

Clay	2θ (°)	*d*-spacing (Å)
UNT	7.26	12.16
B-TC	3.04	29.04
C-TC	3.90	22.64
H-TC	3.80	23.23

UNT showed a peak at 7.26° corresponding to the (001) plane, having an interlayer spacing of 12.16 Å. The interlayer spacing for the treated clays was broadened as organic modifiers came to reside between the silicate layers; a shifting of the peak to lower 2θ values was shown. Among all the intercalating agents used, B-TC was found to display the highest spacing value (~30 Å), which was due to the higher alkyl chain length.

TGA was used to confirm the presence of organic molecules. The high thermal stability of the organoclays was important for further dispersion (exfoliation) of the clay in the polymer matrix. From TGA curves (Fig. 2), it can be seen that UNT showed about a 5 wt % loss at 300°C, mostly because of water. B-TC showed a 20 wt % loss, H-TC showed a 15 wt % loss, and C-TC showed a 6–7 wt % loss at 300°C because of the loss of water or gases and the degradation of organic molecules. Among the three treated clays, C-TC showed high thermal stability. Because of their aromatic ring structure, pyridinium cations have more thermal stability than ammonium cations.

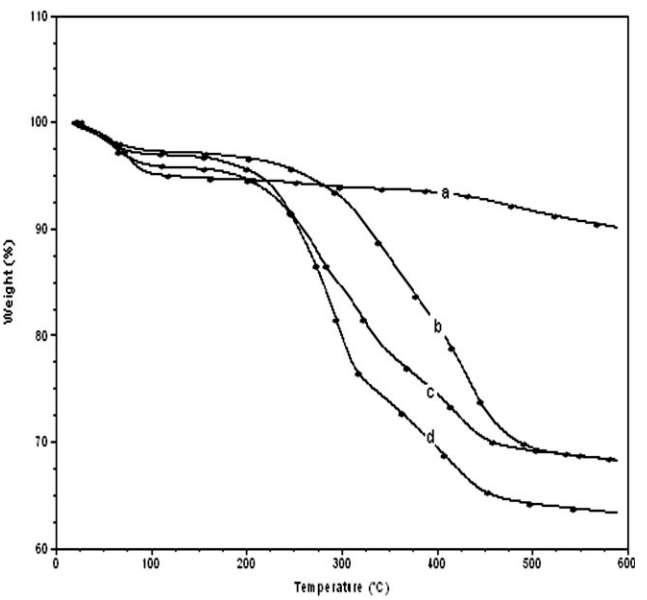

Figure 2 TGA of (a) UNT, (b) C-TC, (c) H-TC, and (d) B-TC.

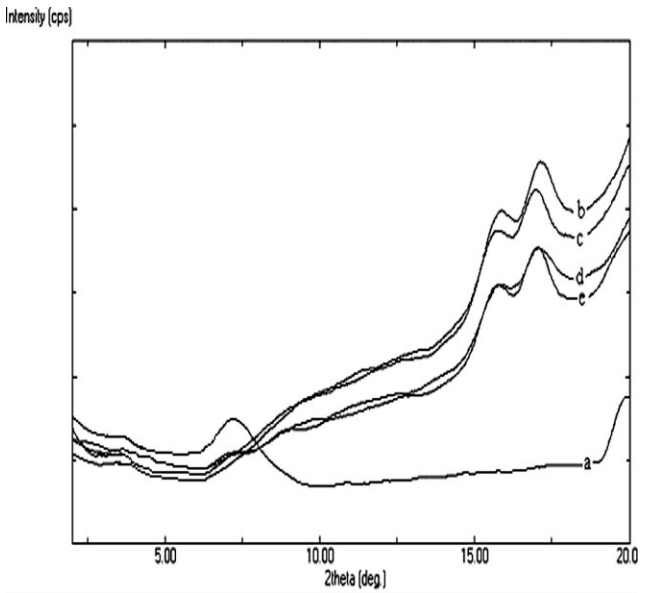

Figure 3 XRD patterns of (a) UNT, (b) PBT, (c) PBT/UNT1, (d) PBT/UNT3, and (e) PBT/UNT5.

Dispersability of the organoclay in PBT

The XRD patterns for UNT and its nanocomposites containing 1, 3, or 5 wt % clay are presented in Figure 3. UNT showed a peak at 7.26° corresponding to the (001) plane, having an interlayer spacing of 12.16 Å. PBT/UNT nanocomposites exhibited no peak corresponding to the same interlayer spacing, and this revealed that PBT could not intercalate into the gallery without modification.

The XRD patterns for C-TC and its nanocomposites containing 1, 3, or 5 wt % clay are presented in Figure 4. Intercalated structures were obtained, and they were shown by the presence of a peak at lower 2θ values, resulting in an increased interlayer spacing. PBT/C-TC1 showed a spacing of 35.6 Å at an angle of 2.48°, and this was found to be greater than those of PBT/C-TC3 and PBT/C-TC5, resulting in good mechanical properties due to the proper dispersion. Similarly, XRD patterns for PBT/B-TC and PBT/H-TC nanocomposites containing 1, 3, or 5 wt % clay are presented in Figures 5 and 6, respectively. Intercalated structures were shown in all

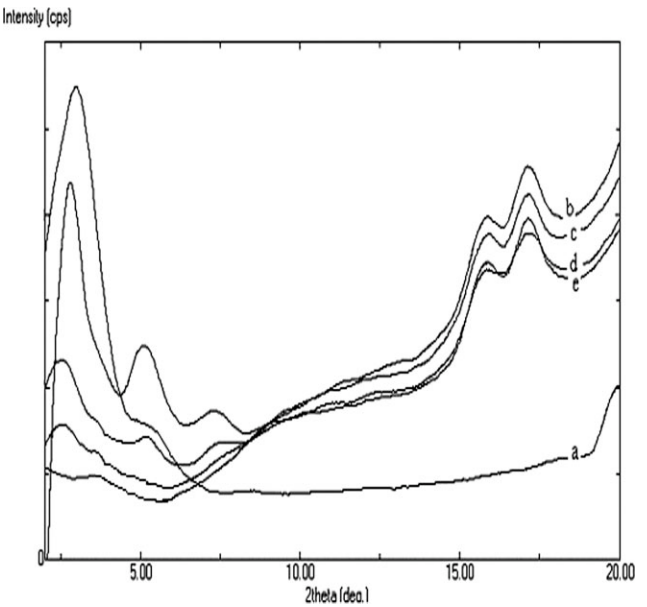

Figure 5 XRD patterns of (a) B-TC, (b) PBT, (c) PBT/B-TC1, (d) PBT/B-TC3, and (e) PBT/B-TC5.

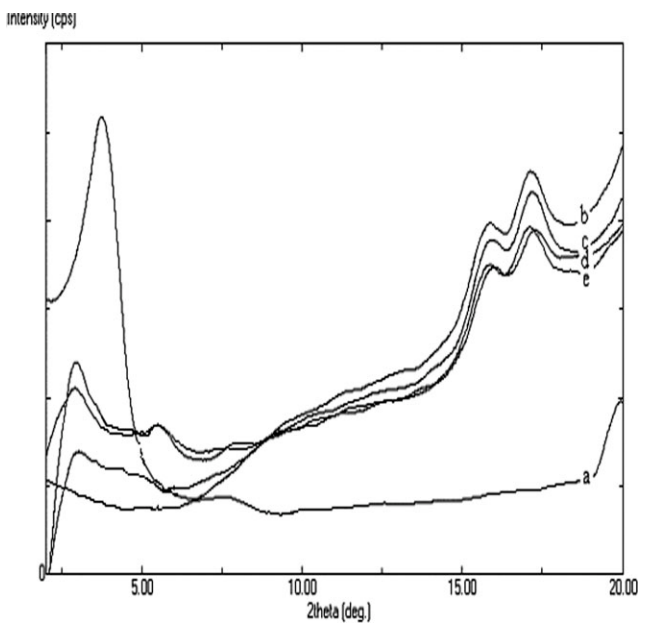

Figure 4 XRD patterns of (a) C-TC, (b) PBT, (c) PBT/C-TC1, (d) PBT/C-TC3, and (e) PBT/C-TC5.

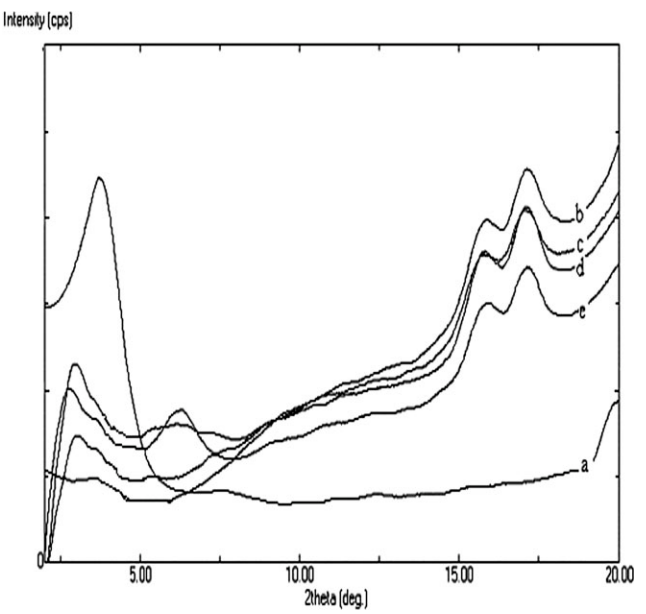

Figure 6 XRD patterns of (a) H-TC, (b) PBT, (c) PBT/H-TC1, (d) PBT/H-TC3, and (e) PBT/H-TC5.

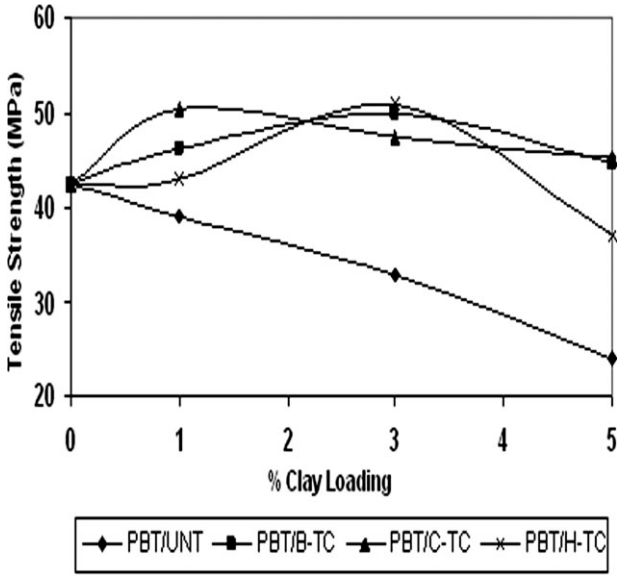

Figure 7 Tensile strength versus the clay loading for the PBT/clay nanocomposites.

these cases. PBT/B-TC1 and PBT/B-TC3 showed a peak at an angle of 2.52° with a spacing of 35.03 Å, which was more than that of PBT/B-TC5. In the case of PBT/H-TC nanocomposites, PBT/H-TC5 showed increased spacing versus that of PBT/H-TC1 and PBT/H-TC3.

Mechanical properties

The PBT/clay nanocomposites containing clay treated with different intercalating agents showed an increase in the tensile strength up to a 3 wt % clay loading for PBT/B-TC and PBT/H-TC and then decreased (Fig. 7). However, in the case of PBT/C-TC, the tensile strength increased up to a 1 wt % clay loading and then decreased. The initial increase was due to good intercalation and exfoliation at lower loadings, but the decrease was due to the clay surface increasing with a higher clay loading, and the polymer available for the clay could not sufficiently wet or exfoliate the clay as the loading increased. The clay treated with different intercalating agents degraded at the processing temperature of PBT, and this resulted in a decrease in the tensile strength. The increase in the tensile strength for PBT/C-TC1 was greater in comparison with PBT/B-TC1 and PBT/H-TC1 because of its lesser degradability at the processing temperature.

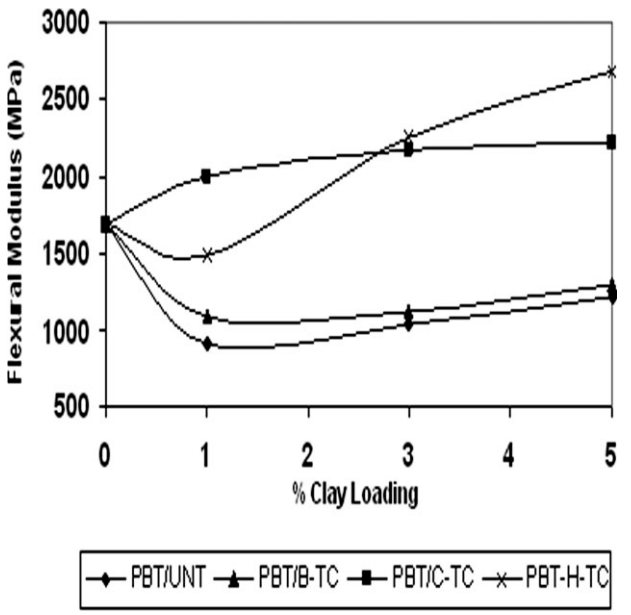

Figure 8 Flexural modulus versus the clay loading for the PBT/clay nanocomposites.

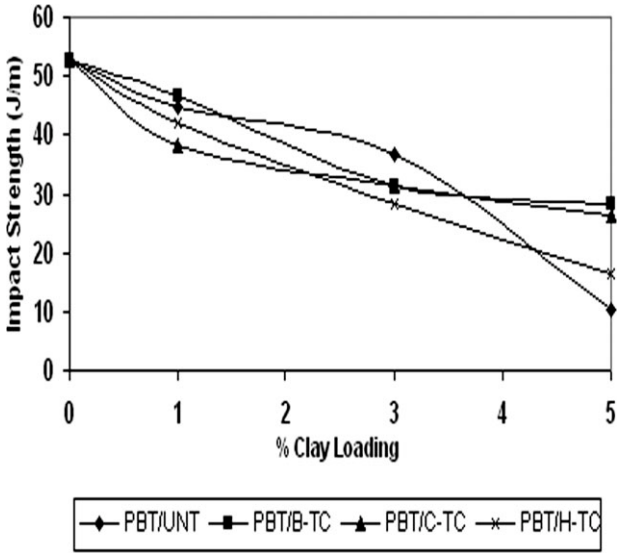

Figure 9 Impact strength versus the clay loading for the PBT/clay nanocomposites.

The flexural modulus of PBT/C-TC increased, but in the case of PBT/B-TC, the flexural modulus decreased at 1% and then increased slightly. PBT/H-TC1 showed a decrease in the flexural modulus, which may have been due to an insufficient amount of clay for sufficient rigidity. At a higher clay loading, because a sufficient amount of clay provided sufficient rigidity, an increase in the flexural modulus resulted. The increase in the flexural modulus indicated an increase in the rigidity of the nanocomposites at the same deformation level (Fig. 8). With an increase in the clay loading, the impact properties of the PBT nanocomposites decreased (Fig. 9). This decrease was due to a lack of impact energy absorption, transfer, and dissipation, which may have been due to poor interfacial bonding between the clay and polymer. The increased amount of filler restricted the mobility of matrix molecules, resulting in decreased impact strength.

TABLE III
DSC Data for the PBT/Clay Nanocomposites

	Melting				Crystallization	
Composition	Onset (°C)	T_m (°C)	Crystallinity (%)	Increase or decrease in crystallinity (%)	Onset (°C)	T_c (°C)
PBT	205.4	222.83	26.37	—	202.64	189.66
PBT/UNT1	205.96	224.24	29.65	+3.28	205.37	192.73
PBT/B-TC1	206.2	223.06	27.40	+1.03	203.64	190.84
PBT/C-TC1	206.29	224.12	25.72	−0.65	203.16	190.48
PBT/H-TC1	206.5	223.28	26.91	+0.54	202.83	189.98
PBT/UNT3	206.16	223.90	21.40	−4.97	202.68	189.66
PBT/B-TC3	206.07	222.17	29.98	+ 3.61	205.85	193.09
PBT/C-TC3	206.16	222.47	23.30	−3.07	202.43	189.46
PBT/H-TC3	206.37	224.19	29.76	+3.39	207.9	195.33
PBT/UNT5	207.06	224.49	26.18	−0.19	207.56	194.97
PBT/B-TC5	205.42	223.45	32.22	+5.85	204.11	191.20
PBT/C-TC5	206.34	222.72	27.07	+0.7	205.07	192.25
PBT/H-TC5	208.24	225.06	29.96	+3.59	207.22	194.68

Thermal properties of the PBT/clay nanocomposites

The T_m and T_c values determined from DSC measurements are presented in Table III. Figures 10–15 represent the DSC results for PBT/clay nanocomposites containing UNT and treated clays (1, 3, or 5 wt %). The incorporation of clay did not have a significant effect on the T_m values of the nanocomposites. There was an increase in the T_c and crystallinity values of the PBT/clay nanocomposites because of the tendency of clay to act as a nucleating agent on account of the small particle size and high surface area of silicate platelets and their chemical affinity for the polymer, which induced a nucleation and lamellar ordering effect. The addition of organoclay produced a maximum increase of about 6% in the crystallinity for PBT/B-TC5. The increase in the crystallinity was possible because of the smaller size of the treated clay particles, which provided more heterophase nuclei to increase the crystallinity. However, the decrease in the crystallinity may have been due to the large size of the crystallite or crystallites, which could coalesce, developing the stresses at the interface and affecting the crystallinity.

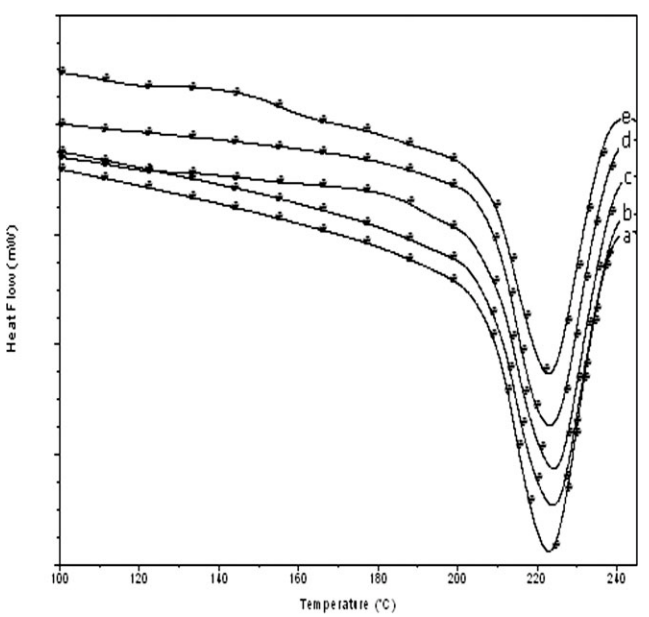

Figure 10 DSC heating thermograms of (a) PBT/B-TC1, (b) PBT/C-TC1, (c) PBT/UNT1, (d) PBT/H-TC1, and (e) PBT.

CONCLUSIONS

Organic modification of clay is necessary to generate nanocomposites by melt compounding. In this study, clay was organically modified, and a series of nanocomposites composed of PBT and organoclay

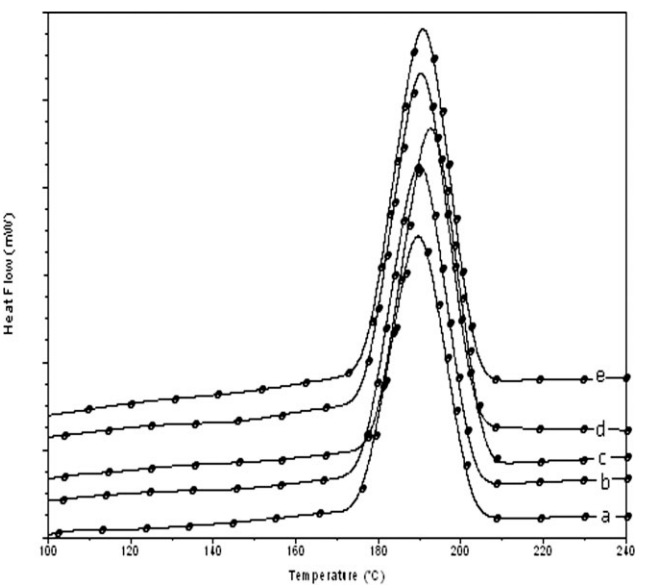

Figure 11 DSC cooling thermograms of (a) PBT, (b) PBT/H-TC1, (c) PBT/UNT1, (d) PBT/C-TC1, and (e) PBT/B-TC1.

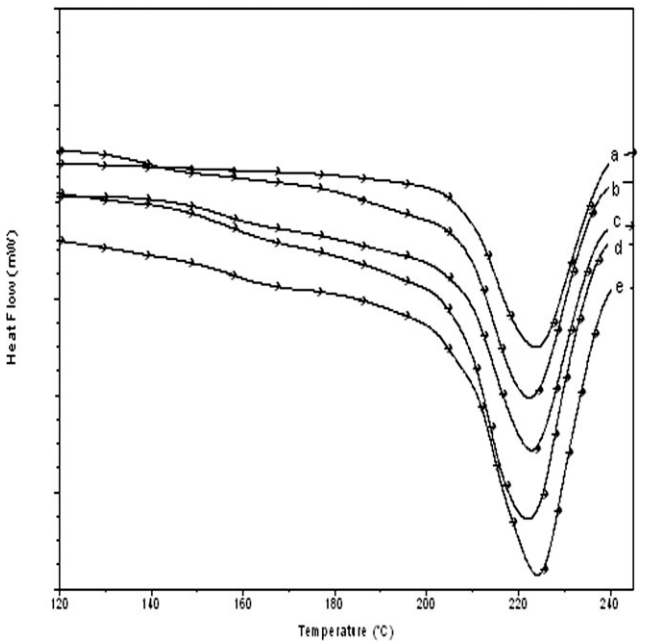

Figure 12 DSC heating thermograms of (a) PBT/UNT3, (b) PBT/C-TC3, (c) PBT, (d) PBT/B-TC3, and (e) PBT/H-TC3.

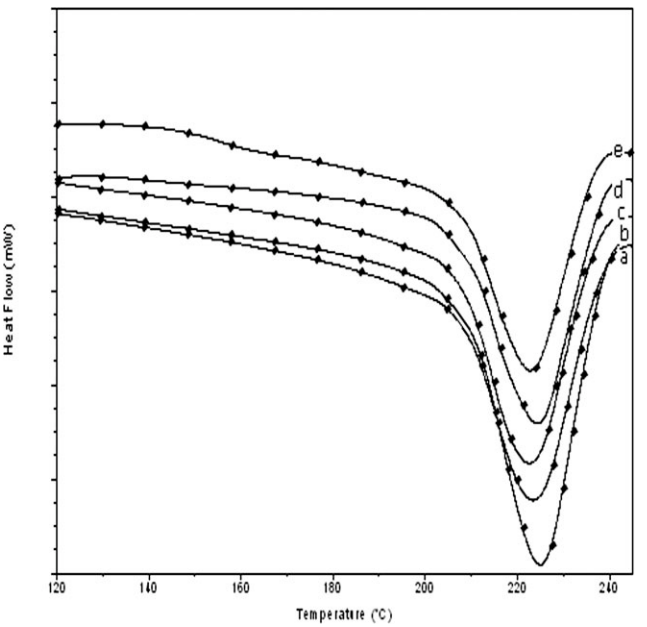

Figure 14 DSC heating thermograms of (a) PBT/B-TC5, (b) PBT/H-TC5, (c) PBT/C-TC5, (d) PBT/UNT5, and (e) PBT.

were successfully prepared through a melt intercalation approach. C-TC showed high thermal stability because of pyridinium cations. As they were characterized with various techniques, the resulting mechanical and thermal properties were found to be sensitive to the nanocomposite structure and clay content. The PBT/C-TC nanocomposites showed better overall mechanical properties than PBT/B-TC and PBT/H-TC, and this was supported by the XRD study. Overall, it was found that the addition of a small amount of organoclay (up to 3 wt %) was enough to improve the mechanical properties of PBT. The addition of organoclay affected the crystallinity of the polymer because of the tendency of clay to act as a nucleating agent; this was shown by DSC studies.

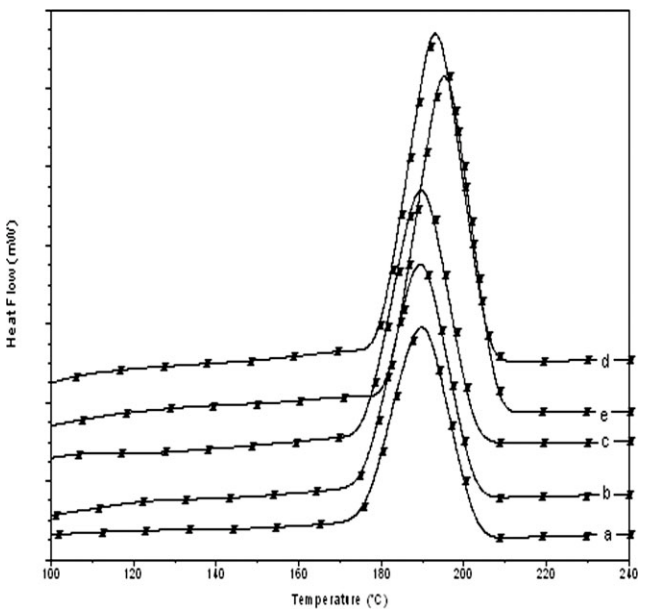

Figure 13 DSC cooling thermograms of (a) PBT/UNT3, (b) PBT/C-TC3, (c) PBT, (d) PBT/B-TC3, and (e) PBT/H-TC3.

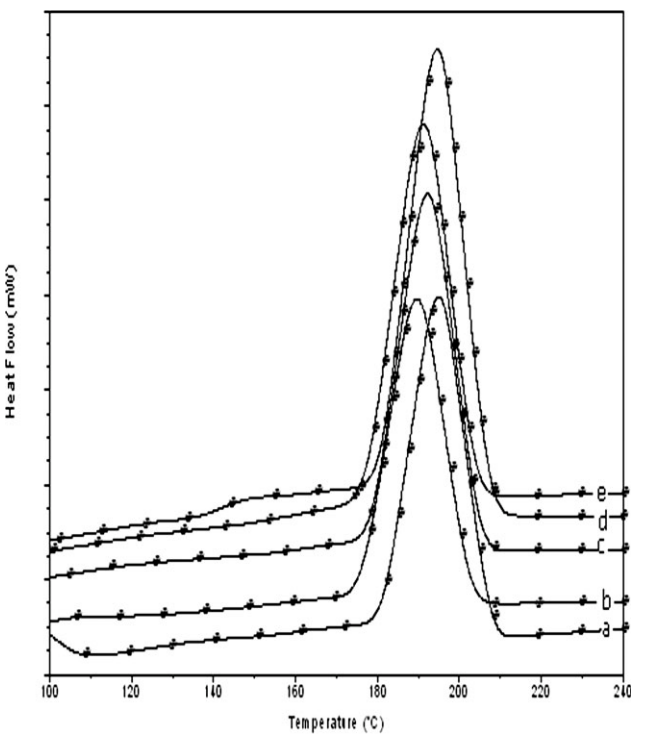

Figure 15 DSC cooling thermograms of (a) PBT/UNT5, (b) PBT, (c) PBT/C-TC5, (d) PBT/H-TC5, and (e) PBT/B-TC5.

References

1. Karak, N. J Polym Mater 2006, 23, 1.
2. Zhang, J.; Wilkie, C. A. Polym Degrad Stab 2003, 80, 163.
3. Yeh, J. M.; Chen, C.-L. J Appl Polym Sci 2006, 99, 1576.
4. Agag, T.; Koga, T. Polymer 2001, 42, 3399.
5. Lia, L.; Qi, Z.; Zhu, X. J. J Appl Polym Sci 1999, 71, 1133.
6. Zhao, C.; Qin, H. Polym Degrad Stab 2005, 87, 183.
7. Sanchez-Solis, A.; Esterada, M. R. Polym Eng Sci 2004, 44, 1094.
8. Ou, C. F.; Ho, M. T. J Appl Polym Sci 2004, 91, 140.
9. Lee, A.; Lichtenhan, J. D. J Polym Sci Part A: Polym Chem 1999, 37, 2225.
10. Lee, J. W.; Lim, Y. T.; Park, O. O. Polym Bull 2000, 45, 191.
11. Chen, G.; Liu, S.; Chen, S.; Qi, Z. Macromol Chem Phys 2001, 202, 1189.
12. Suh, D. J.; Lim, Y. T.; Park, O. O. Polymer 2000, 41, 8557.
13. Domenico, A. Polym Eng Sci 2004, 44, 1012.
14. Xiao, J.; Tang, Y.; Hu, Y. Eur Polym J 2005, 41, 1030.
15. Anand, J. S. Application of Plastics; CIPET: Chennai, India, 1997.